Suggestion of a "Twist" Mechanism in the Oligomerisation of a Dimeric Phospha(III)zane: Insights into the Selection of Adamantoid and Macrocyclic Alternatives

Alan Bashall,[b] Emma L. Doyle,[a] Felipe García,[a] Gavin T. Lawson,[a] David J. Linton,[a] David Moncrieff,[c] Mary McPartlin,[b] Anthony D. Woods,[a] and Dominic S. Wright*[a]

Abstract: The reaction of the dimeric phospha(III)zane $[ClP(\mu\text{-Npy})]_2$ (**1**) (py = 2-pyridyl) with pyNHLi (2:1 equivalents, respectively) in THF/Et_3N leads to rapid formation of the bicyclic nona-phospha(III)zane $[\{ClP(Npy)_2\}_2\text{-}\{P_2(Npy)\}]$ (**2**). This novel rearrangement can be rationalised by a mechanism involving "twisting (or swivelling)" of the central P(μ-Npy)P fragment of the presumed intermediate $[\{ClP(\mu\text{-Npy})_2P\}_2(\mu\text{-Npy})]$ (**3**), a process that provides a fundamental mechanistic relationship between the majority of previously reported imidophosphospha(III)zanes. This process is fundamentally reliant on relief from ring strain on going from the four-membered ring units of **3** to the six-membered units of **2**. The rearrangement observed for **1** is suppressed on steric grounds by Me-substitution of the pyridine ring at the 6-position, the dimeric phosphazane $[ClP(\mu\text{-N-6-Me-py})]_2$ (**4**) (6-Me-py = 6-methyl-2-pyridyl) being formed almost exclusively in the 1:1 reaction of PCl_3 with 6-Me-pyNHLi. The syntheses and X-ray structures of **1**, **2** and **4** are reported, together with ^{31}P NMR spectroscopic and DFT calculational studies of the conversion of models of **1** into **2**. The combined studies pinpoint relief from ring strain as the key factor dictating the rearrangement.

Keywords: density functional calculations · nitrogen · phosphorus · rearrangement

Introduction

The reactions of PCl_3 with primary amines (RNH_2), amine hydrochlorides (RNH_3Cl), amides (RNH^-) or silylamides $[RN(SiR'_3)_2]$ give a range of phospha(III)zane products, depending largely on the steric demands of the organic substituents (R) and the stoichiometry of the reactions. The commonest products are dimers of the type $[ClP(\mu\text{-NR})]_2$ (**A**, Scheme 1),[1] which have been observed mainly with more sterically demanding primary amines. Larger trimeric (**B**)[2] rings have been obtained with less sterically bulky precursors. Also of note are bicyclic (**C**),[2c, 3] adamantoid (**D**)[4] and macrocyclic (**E**)[5] phosphazane cages, which are obtained by a range of synthetic procedures for less sterically demanding organic groups.

Although representative examples of phosphazanes **A** – **E** have been well characterised, few systematic studies have focused on the mechanism of formation of these species and the potential mechanistic relationship between them. In one example, such a mechanistic relationship between a trimeric arrangement **B** and a bicyclic arrangement **C** has been established, the trimer $[ClP(\mu\text{-NMe})]_3$ being converted into the bicyclic compound $[Cl_2P_4(NMe)_5]$ upon reaction with $MeN(SiMe_3)_2$.[6] In addition, the dimer $[\{P(\mu\text{-N}i\text{Pr})\}_2\text{-}(\mu\text{-N}i\text{Pr})]_2$ (of type **E**) was shown to revert to the more thermodynamically stable adamantoid isomer (type **D**) upon thermolysis in the solid state.[5a] Interestingly, the increased steric demands of the organic substituents in the isostructural dimer $[\{P(\mu\text{-N}t\text{Bu})\}_2(\mu\text{-N}t\text{Bu})]_2$ confer greater stability, and the compound does not undergo rearrangement into the adamantoid structure under similar conditions.[5b]

We recently showed that the 1:1 stoichiometric reaction of the dimers $[ClP(\mu\text{-N}t\text{Bu})]_2$ and $[H_2NP(\mu\text{-N}t\text{Bu})]_2$ in the presence of Et_3N leads to the almost quantitative formation of the tetrameric macrocycle $[\{P(\mu\text{-N}t\text{Bu})\}_2(\mu\text{-NH})]_4$[7] [structurally related to the previously reported cyclic dimers $[\{P(\mu\text{-NR})\}_2(\mu\text{-NR})]_2$ (R = *i*Pr, *t*Bu)[5]] (Scheme 2). The selectivity of this cyclisation reaction appears to result partly from preor-

[a] Dr. D. S. Wright, E. L. Doyle, F. García, Dr. G. T. Lawson, D. J. Linton, Dr. A. D. Woods
Chemistry Department, Cambridge University
Lensfield Road, Cambridge CB21EW (UK)
Fax: (+44) 1223-763122
E-mail: dsw1000@cus.cam.ac.uk.

[b] Dr. A. Bashall, Prof. M. McPartlin
School of Chemistry, University of North London
London N78DB (UK)

[c] Dr. D. Moncrieff
School of Computational Science Information and Technology
Florida State University, Tallahassee, FL 32306 (USA)

  0947-6539/02/0824-5723 $ 20.00+.50/0

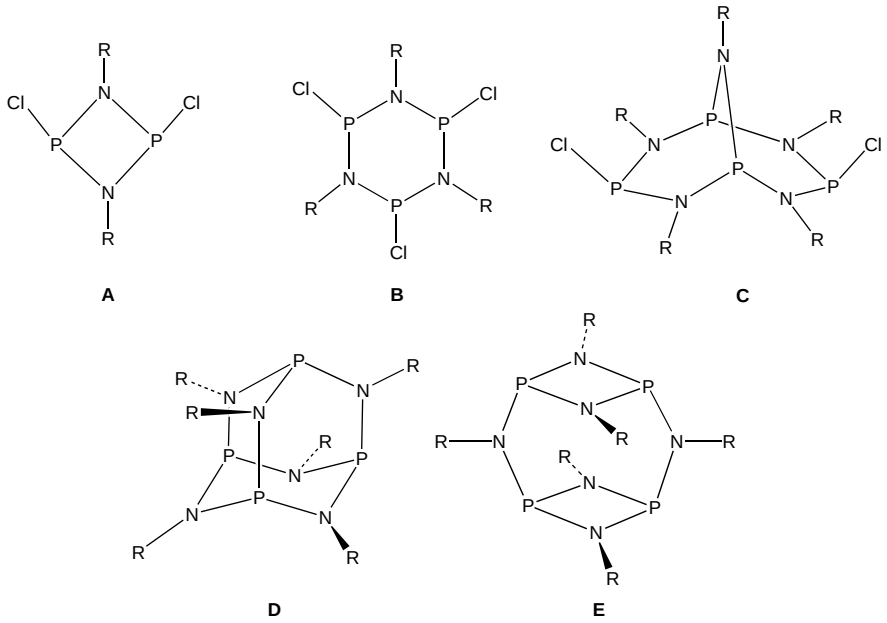

Scheme 1. Major structural types identified for imidophospha(III)zanes.

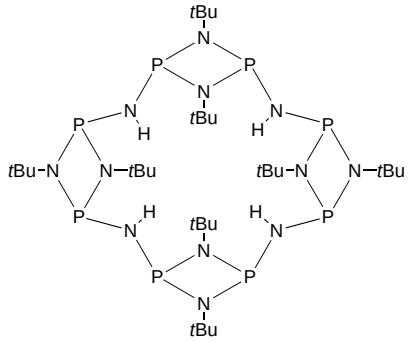

Scheme 2. Structure of the tetrameric macrocycle $[\{P(\mu\text{-N}t\text{Bu})\}_2(\mu\text{-NH})]_4$.

ganisation of the dimeric precursors, both of which prefer *cis* conformations in the solid state and in solution. However, the isolation of minor amounts of the host–guest adduct $[\{P(\mu\text{-N}t\text{Bu})\}_2(\mu\text{-NH})]_5\cdot HCl$ from this reaction (containing a macrocyclic pentamer) may also indicate that templating by Cl^- anions provides an additional factor favouring cyclisation.[8] Our interest in extending this synthetic approach to other macrocycles of the type $[\{P(\mu\text{-NR})\}_2(\mu\text{-NH})]_n$ has led us to explore the synthesis of a broad range of dimers of the type $[ClP(\mu\text{-NR})]_2$ (the fundamental starting materials for cyclisation). We present here a study of the synthesis of the dimer $[ClP(\mu\text{-Npy})]_2$ (**1**) (py = 2-pyridyl) and the observation of its surprising rearrangement into the bicyclic complex $[Cl_2P_4(Npy)_5]$ (**2**) in the presence of pyNHLi/Et_3N. This observation, and the suppression of the rearrangement in the case of the dimer $[ClP(\mu\text{-N-6-Me-2-py})]_2$ (**4**) (6-Me-2-py = 6-methyl-2-pyridyl), provide a key to the relationship between many of the imidophosphazane structural types previously observed.

Results and Discussion

Synthesis and X-ray structures: One target of our ongoing synthetic studies of macrocycles of the type $[\{P(\mu\text{-NR})\}_2(\mu\text{-NH})]_n$ is the preparation of species containing donor functionality within their organic substituents (R). However, comparatively few of the dimers $[ClP(\mu\text{-NR})]_2$ (the necessary starting materials for these studies) have been fully characterised previously and only one of these species has donor functionality present within the organic substituent.[1e] Pyridyl (py) substituents seemed to us to be particularly suitable for this purpose since their low steric demands should allow relatively unhindered rotation within the dimeric constituents of the macrocyles, therefore facilitating the coordination of their donor N centres to metal ions within the macrocyclic cavities.

Pilot studies in this area concentrated on 2-pyridyl amine substituents (pyN). Several synthetic approaches based on conventional literature procedures were investigated, including: i) reaction of 2-pyNH$_2$ with PCl_3 in THF, in the presence of Et_3N as the Brønsted base; ii) reaction of pyNH$_2$ with PCl_3 as the solvent. Both of these methods proved ineffective and only intractable solids were obtained. Finally, a procedure based on that developed by Roesky et al. in the synthesis of $[ClP(\mu\text{-NDipp})]_2$ (Dipp = 2,4,6-$(CF_3)_3C_6H_2$) was adopted,[1d] in order to minimise the likely complication of the pyridyl substituent behaving as a Brønsted base. Accordingly, PCl_3 was treated with pyNHLi (1:1 equivalents) in THF/Et_3N at $-78\,^\circ C$. However, following extraction and crystallisation of the product with toluene, the phosphazanes $[ClP(\mu\text{-Npy})]_2$ (**1**) and $[Cl_2P_4(Npy)_5]$ (**2**·toluene) are both obtained (Scheme 3) (see Experimental Section). Compounds **1** and **2** can be separated by careful fractional crystallisation from solutions of the crude extract in toluene, with **1** being crystallised in the

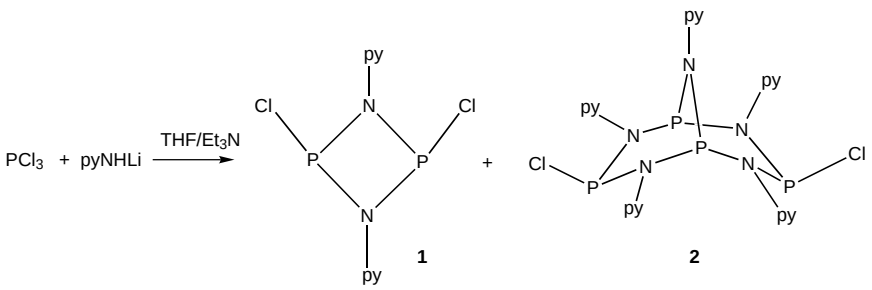

Scheme 3. Formation of phosphazanes $[ClP(\mu\text{-Npy})]_2$ (**1**) and $[Cl_2P_4(Npy)_5]$ (**2**).

0947-6539/02/0824-5724 $ 20.00+.50/0 *Chem. Eur. J.* **2002**, *8*, No. 24

first batch and **2** being obtained as the major component of the second batch (which is normally contaminated with **1**). Both compounds were initially characterised by elemental analysis and by IR, ^{1}H and ^{31}P NMR spectroscopy. The ^{31}P NMR chemical shift for **1** at room temperature (a singlet at $\delta = 178.5$) is particularly diagnostic, the value being similar to that found for other dimers of the type $[ClP(\mu\text{-}NR)]_2$ (e.g., R = *t*Bu, $\delta = 207.6$). Two triplets are observed in the room-temperature ^{31}P NMR spectrum of **2** in toluene [$\delta = 108.4$ (P–Cl) and $\delta = 64.6$; $J(PNP) = 7.3$ Hz], indicating that only one conformational isomer of **2** is present in solution. The low value of the P–P coupling constant (J(PNP)) in cages of this type has been attributed to the *transoid* orientation of the P lone pairs within the cage.[3] The room-temperature ^{1}H NMR spectrum of **2** exhibits pairs of related, complex multiplets (relative ratio 1:4) in the aromatic region. Presumably, these pairs correspond to the two py ligand environments within the eight-membered ring unit (4py) and the bridgehead (1py).

In an attempt to suppress the formation of the bicyclic framework, the reaction was performed using 6-Me-2-pyNH-Li (6-Me-2-py = 6-methyl-2-pyridyl) under similar conditions. The ^{31}P NMR spectrum of the crude toluene extract from this reaction reveals that the dimer $[ClP(\mu\text{-N-6-Me-py})]_2$ (**4**) is formed almost exclusively (Scheme 4). Only a minor amount

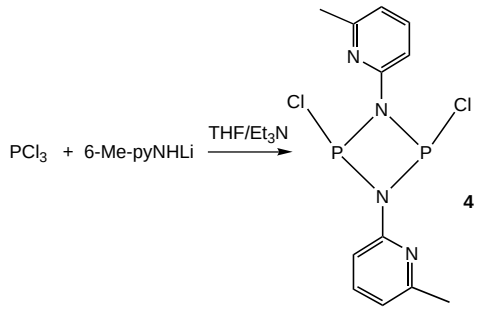

Scheme 4. Formation of dimer $[ClP(\mu\text{-N-6-Me-py})]_2$ (**4**).

of the presumed bicyclic product could be identified in this mixture ($\delta = 109.0$ (t), 62.7 (t)). Compound **4** can be isolated in a highly pure form by solvent reduction of the crude extract under vacuum, followed by crystallisation at room temperature (see Experimental Section). As in the case of **1**, the ^{31}P NMR chemical shift of **4** (a singlet at $\delta = 182.0$) provided an initial, strong indication of the formation of a dimeric framework.

X-ray crystallographic studies were undertaken on **1**, **2**·toluene and **4**. Details of the crystal data and structure refinements are given in Table 1. Table 2 lists key bond lengths and angles for the dimers **1** and **4** and Table 3 gives the corresponding data for the bicyclic complex **2**.

The structures of the dimers **1** (Figure 1) and **4** (Figure 2) are as anticipated, both being composed of four-membered, virtually planar P_2N_2 rings (maximum deviation 0.02 Å in both complexes). The P–N bonds [range 1.711(3) – 1.723(3) Å] and P–N–P [100.4(7) – 100.8(7)°] and N–P–N [79.3(1) – 79.4(1)°] angles within these ring units are very similar for both compounds and typical of dimeric imidophosphazanes.[1] The

Table 1. Crystal data and refinements for $[ClP(\mu\text{-Npy})]_2$ (**1**), $[Cl_2P_4(Npy)_5]$·toluene (**2**·toluene) and $[ClP(\mu\text{-N-6-Me-py})]_2$ (**4**).

Compound[a]	**1**	**2**·toluene	**4**
empirical formula	$C_{10}H_8Cl_2N_4P_2$	$C_{32}H_{28}Cl_2N_{10}P_4$	$C_{12}H_{12}C_{l2}N_4P_2$
M_W	317.04	747.42	345.10
crystal system	monoclinic	triclinic	monoclinic
space group	$P2_1/n$	$P\bar{1}$	$P2_1/c$
T [K]	223(2)	203(2)	180(2)
unit cell parameters			
a [Å]	9.237(4)	11.005(5)	10.0421(2)
b [Å]	12.327(3)	11.687(4)	12.0631(3)
c [Å]	12.743(3)	14.462(4)	13.0545(3)
a [°]	—	73.04(2)	—
b [°]	104.76(2)	86.71(3)	104.277(2)
g [°]	—	78.96(5)	—
U [Å^3]	1403.0(7)	1746.1(11)	1532.56(6)
Z	4	2	4
ρ_{calcd} [Mg m^{-3}]	1.501	1.422	1.496
μ [mm^{-1}]	0.677	0.410	0.626
independent reflections	1943	4815	3506
R_{int}	0.022	0.043	0.029
R indices [$I > 2\sigma(I)$], $R1$	0.038	0.060	0.031
$WR2$	0.076	0.137	0.078
R indices (all data), $R1$	0.060	0.127	0.039
$WR2$	0.150	0.189	0.082

Table 2. Selected bond lengths and angles for the dimers $[ClP(\mu\text{-NR}]_2$ [R = py (**1**), 6-Me-py (**4**)].

	1	**4**
	bond lengths [Å]	
P(1)–N(1)	1.721(3)	1.714(1)
P(1)–N(2)	1.711(3)	1.707(1)
P(2)–N(1)	1.711(3)	1.703(1)
P(2)–N(2)	1.723(3)	1.722(1)
P(1)–Cl(1)	2.095(2)	2.1073(6)
P(2)–Cl(2)	2.108(2)	2.1003(6)
C(11,21)–N(1,2)	mean 1.403	mean 1.400
C(11,21):N(12,22)	mean 1.338	mean 1.332
	angles [°]	
P(1)–N(1)–P(2)	100.7(2)	100.82(7)
P(1)–N(2)–P(2)	100.6(2)	100.35(7)
N(1)–P(1)–N(2)	79.4(1)	79.41(7)
N(1)–P(2)–N(2)	79.3(1)	79.31(6)
N–P–Cl	mean 102.5	mean 102.5
max. P_2N_2 ring deviation	0.02	0.02

Table 3. Selected bond lengths and angles for bicyclic $[Cl_2P_4(\mu\text{-Npy})_5]$ (**2**).

	bond lengths [Å]		
P(1)–N(1)	1.707(5)	P(3)–N(1)	1.755(6)
P(1)–N(4)	1.716(6)	P(3)–N(3)	1.748(5)
P(1)–Cl(1)	2.147(3)	P(3)–N(5)	1.729(6)
P(2)–N(2)	1.692(5)	P(4)–N(2)	1.754(6)
P(2)–N(3)	1.725(5)	P(4)–N(4)	1.737(5)
P(2)–Cl(2)	2.138(3)	P(4)–N(5)	1.708(5)
	angles [°]		
N–P–N range	94.8(3) – 99.8(2)	P–N–P range	125.2(3) – 128.6(3)
N–P–Cl mean	100.1	ΣN range	354.9 – 360.0

cis conformation of the Cl atoms with respect to the P_2N_2 units in both compounds is also typical of the majority of imidophosphazane dimers of this type[1] and is reassuring with respect to their potential applications as precursors for the target functionalised macrocycles. The pyridyl ring units in

  0947-6539/02/0824-5725 $ 20.00+.50/0

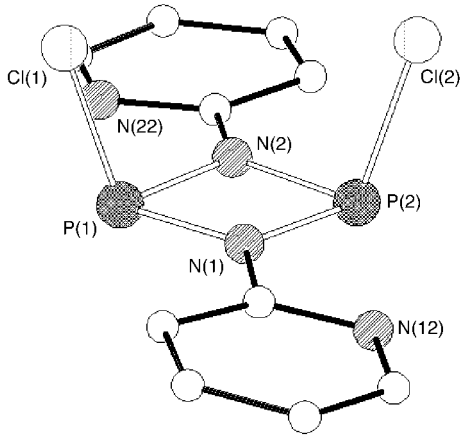

Figure 1. Structure of dimeric **1**.

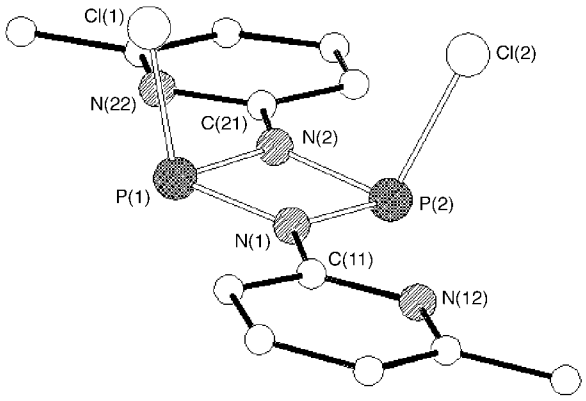

Figure 2. Structure of dimeric **4**.

1 and **4** lie almost in the same plane as the P_2N_2 rings, but are tilted slightly in opposite directions (dihedral angle between the pyridyl rings 10.2° in **1** and 9.4° in **4**). This arrangement is similar to the phenyl rings in $[ClP(\mu\text{-}NPh)]_2$.[1a]

Cage molecules of **2** are composed of a P_4N_5 core, which adopts a bicyclo-1,3,3-nonane arrangement (Figure 3). In addition, there is one molecule of toluene in the lattice per molecule of **2**. The two fused P_3N_3 rings making up this structure of **2** adopt twisted, half-chair conformations, with the P–Cl bonds being orientated towards N(5), the bridgehead 2-pyN group. The P–N bonds fall over a slightly larger range [1.707(5) – 1.755(6) Å] than those found in the dimers **1** and **4**. However, there is no discernible pattern in the P–N bond lengths within the P_4N_5 core of **2**. The P–N–P [range 125.2(3) – 128.6(3)°] and N–P–N [range 94.8(3) – 99.2(2)°] angles within **2** are considerably greater than the corresponding angles in **1** and **4**, indicating that relief from ring strain may underpin the formation of the bicyclic framework from dimeric **1**. Although three compounds containing the same P_4N_5 core structure have been structurally characterised previously, none of these are directly comparable to **2** since all examples in which the cage is not coordinated to a metal centre are partially or completely oxidised at one or more of the P atoms.[3] The P–N bonds are therefore generally shorter (i.e., 1.664(2) – 1.707(2) Å[3]) than in **2**. In contrast, the P–N–P and N–P–N angles in **2** are very similar to those found in the previous examples.[3] The distorted, trigonal-planar geometries of the N centres in **2** are typical of related P_4N_5 cages of this type, the sum of angles about the N centres falling in the range 354.9 – 360.0°.

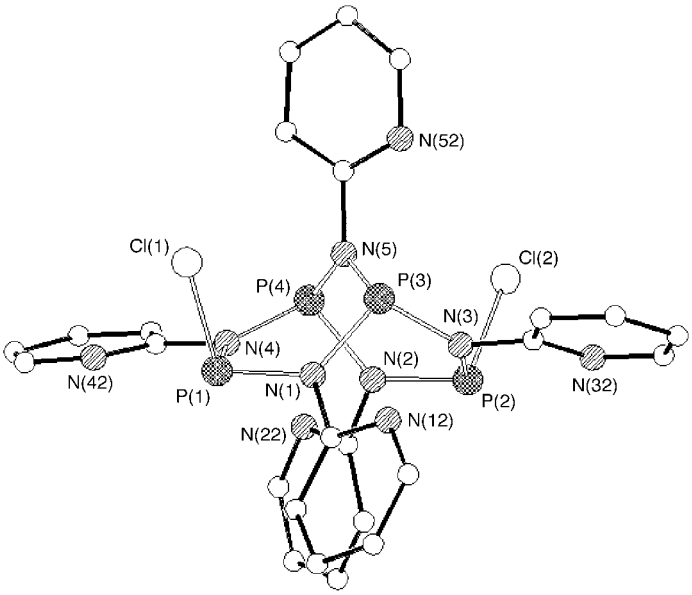

Figure 3. Structure of the bicyclic cage **2**.

The mechanism of selection of macrocyclic and adamantane alternatives: We were intrigued by the formation of the apparently unrelated phosphazane frameworks of **1** and **2** and wondered whether a mechanistic relationship might exist between them. In order to determine this, the reaction of **1** (1 equivalent) with pyNHLi (0.5 equivalents) in THF/Et_3N was monitored by ^{31}P NMR spectroscopy (Figure 4). The addition of pyNHLi/Et_3N to a solution of **1** at −78 °C results in immediate formation of **2** (Figure 4a – c), together with an intermediate **3**, which is characterised by two poorly resolved doublets (at $\delta = 158.2$ and 121.1). The values of the chemical shifts observed for **3** suggest that the two phosphorus environments present in this species are similar to those found in **2**. In addition, the coupling constant for **3** (ca. 33 Hz) is consistent with a (^2J) P–N–P linkage. Holding the reaction mixture at −78 °C for four hours results in an increase in the amount of this intermediate relative to **2** (Figure 4c). Allowing the reaction mixture to warm from −30 to 70 °C gives **2** together with other minor unidentified products (Figure 4d – f).

The exact mechanism by which **1** is converted into **2** is still open to debate. However, the involvement of the trimer $[ClP(\mu\text{-}Npy)]_3$[6] as an intermediate in this reaction appears unlikely, since there is no obvious pathway by which **1** could be converted into this species. A more plausible mechanism involves the formation of the chain isomer of **2**, $[\{ClP(\mu\text{-}Npy)P\}_2(\mu\text{-}Npy)]$ (**3**), by simple oligomerisation of the dimer constituents of **1**, followed by "twisting" of the central $P(\mu\text{-}Npy)_2$ fragment (Scheme 5). Interestingly, it has been shown previously that the reaction of PCl_3 with $PhNH_2$ ultimately results in the formation of a related chain product $[(PhNH)P(\mu\text{-}NPh)_2P]_2(\mu\text{-}NPh)$, by a stepwise pathway from the dimeric diazadiphosphazane $[(PhNH)P(\mu\text{-}NPh)]_2$.[1b] In

  0947-6539/02/0824-5726 $ 20.00+.50/0 *Chem. Eur. J.* **2002**, *8*, No. 24

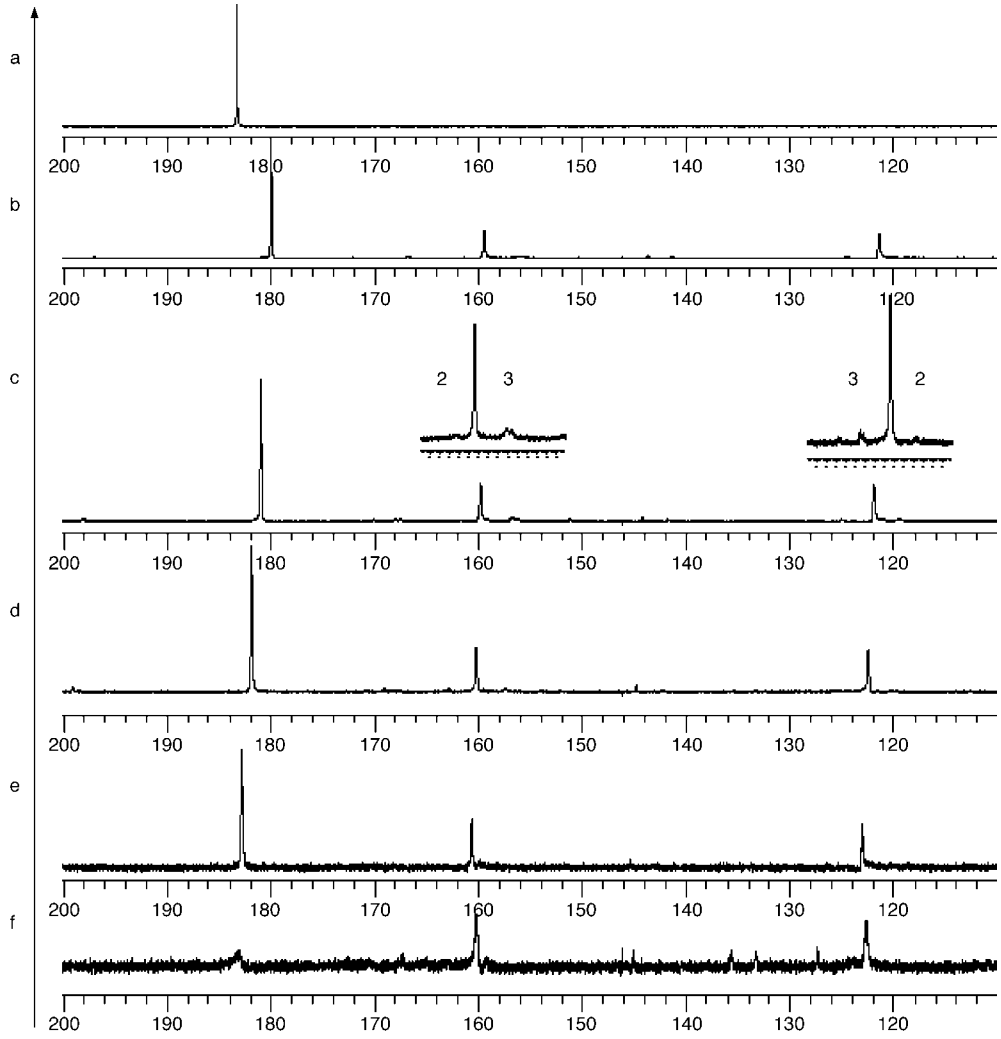

Figure 4. Variable-temperature ^{31}P NMR spectroscopic study of the reaction of **1** with pyNHLi/Et_3N in THF [a) **1**, −78 °C; b) +pyNHLi/Et_3N, −78 °C; c) −78 °C, 4 h; d) −10 °C; e) 25 °C; f) 70 °C].

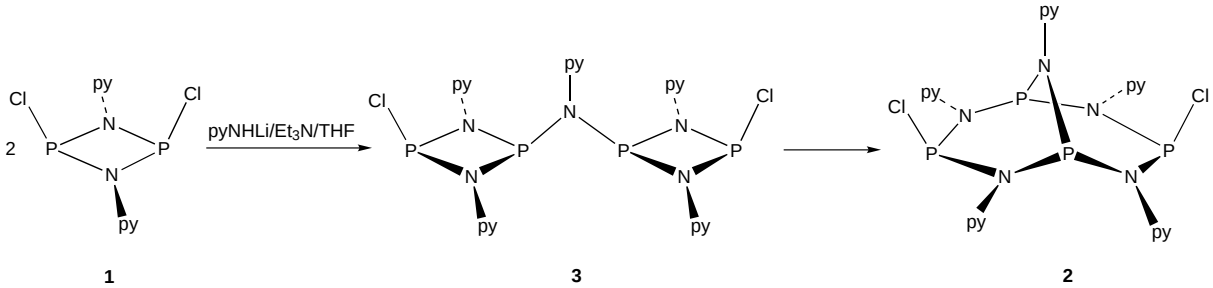

Scheme 5. The formation of [{ClP(μ-Npy)P}$_2$(μ-Npy)] (**3**) and **2**.

addition, the thermal rearrangement of the macrocyclic dimer [{P_2(μ-N*i*Pr)$_2$}$_2$(μ-N*i*Pr)]$_2$ into the adamantoid [P_4(N*i*Pr)$_6$] can be reappraised in the light of the observed conversion of **1** into **2**, as also occurs by a similar "twist" process (Scheme 6).[5a]

A number of factors complicate any attempt to suggest an overall mechanistic scheme that might allow all the principal phospha(III)zane structural types discussed at the beginning of the introduction to this paper to be related to each other. In particular, radically different synthetic procedures have been employed in the preparation of these species. However, a key observation from all previous studies that the structural type obtained is strongly influenced by the steric demands of the organic substituents provides a fundamental indication of thermodynamic control in all of these cases. Combining the observed rearrangement of **1** into **2** with these previous reports[1–5] allows a plausible link between the principal structural types to be proposed, the overall scheme being shown in Figure 5. Depending on the steric demands of the organic substituent (R), dimers (**A**) and/or trimers (**B**) can

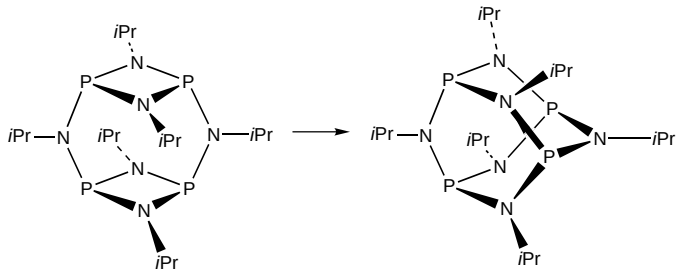

Scheme 6. The rearrangement of the macrocyclic dimer $[\{P_2(\mu\text{-}N\textit{i}Pr)_2\}_2(\mu\text{-}N\textit{i}Pr)]_2$ into the adamantoid $[P_4(N\textit{i}Pr)_6]$ by a "twist" process.

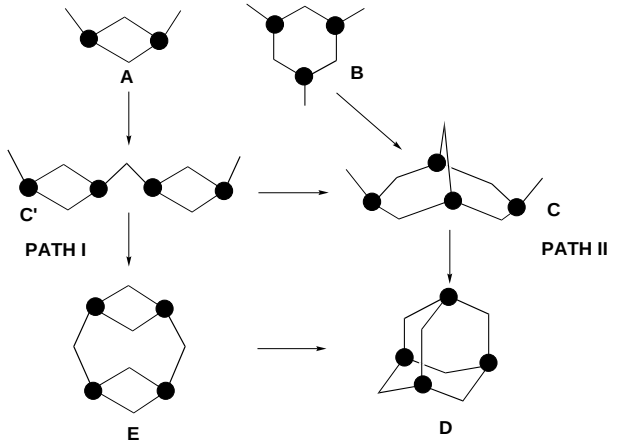

Figure 5. Proposed scheme relating the common types of imidophospha(III)zane structures.

result initially, for example, from the reactions of PCl_3 with RNH_2. The formation of the larger six-membered ring of **B** is favourable only where the organic groups have relatively low steric demands (e.g., Et or Me[2]), since the space available for the accommodation of these groups decreases with increased ring size. The formation of dimers in the majority of cases results from the desire to minimise steric congestion, since a four-membered ring unit maximises the space available for more sterically demanding groups.[1] However, minimising steric congestion occurs at the expense of increased ring strain in these units.

We suggest that the "twist" mechanism observed for the conversion of **1** and **2** provides the pivotal mechanistic pathway responsible for the ultimate selection of the macrocyclic (**E**) and adamantoid (**D**) alternatives. For sterically demanding substituents, pathway **I** will be followed in which the dimeric units are retained in the intermediate **C′**, leading to the formation of **E**. However, for less sterically demanding groups (such as py) relief from ring strain results in rearrangement of **C′** into the isomeric bicyclic structure (**C**), in which the organic substituents can be accommodated within its fused six-membered ring constituents. Although, to our knowledge, no representative examples of the conversion of a bicyclic cage (**C**) into an adamantoid (**D**) have been reported previously, this process appears highly likely on the basis of related studies. Specifically, it has been shown that the P_4N_5 cores of uncoordinated cages are conformationally flexible and that such cages can readily be coordinated to transition metals (TM) using their wing-tip P atoms as donor centres.[3b] This process results in the formation of adamantane-like cage structures containing P_4N_5TM cores. Alternatively, as shown by Scherer et al., collapse of the macrocylic arrangement (**E**) into the adamantane isomer (**D**) can also occur,[5a] provided the organic groups (R) are not too sterically demanding.[5b] It should be noted also that in one case a trimer (**B**) has been shown to be a precursor for a bicyclic structure (**C**).[6]

In order to provide further insights into the ways in which steric factors and ring strain influence the structural arrangement adopted, ab initio calculations were performed in an effort to understand the energetics involved in the isodesmic rearrangement of the chain isomer (**C′**) to the bicylic isomer (**C**) (Scheme 7). This rearrangement is a pivotal one in the proposed pathways outlined in Figure 5. Hydrogen and methyl substituents (R) were used in the model calculations to simulate the effect of different functional groups. Optimisation and frequency analysis were performed using the Gaussian 98 (G98) software program.[9] Two theoretical models were used to determine the energetics involved in the **C′** to **C** rearrangement: density functional theory (DFT) using the B3LYP functional[10] and a MP2 model. In the DFT/B3LYP model, the INT = ULTRAFINE parameter was employed for the numerical grid whilst in the MP2 model the core orbitals were kept frozen and doubly occupied. Two basis sets were used, cc-pvdz basis[11] and a cc-pvtz basis,[12] which were employed in both theoretical models.

Optimisation and frequency calculations were performed at B3LYP/cc-pvdz, B3LYP/cc-pvtz and MP2/cc-pvdz on **C′** and **C** when R = H, while for $R = CH_3$, only the B3LYP model combined with both basis sets was employed. The optimised structures of **C′** and **C** obtained from B3LYP/cc-pvdz and MP2/cc-pvdz are in close agreement; bond lengths are within 0.01 Å and angles are within 1° when compared with the P–N cage structures. The only deviation between the two models comes in the P–Cl bond length, for which the MP2 structure gave a shorter bond length over the B3LYP structure in the range 0.02 – 0.04 Å; this is true for both optimised isomers. The effect on changing the basis set (B3LYP model only) is common to both optimised isomers (R = H and CH_3) such

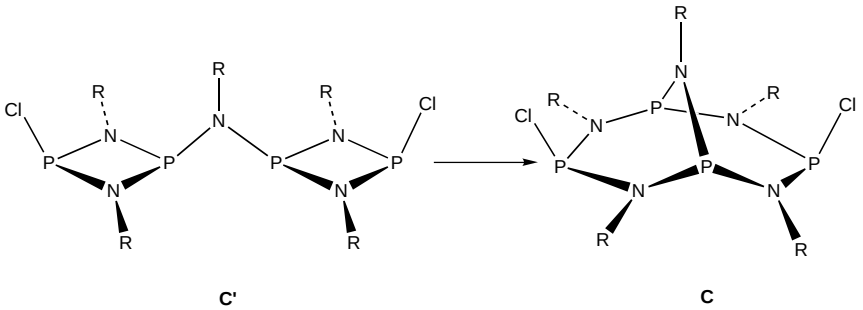

Scheme 7. The rearrangement of the chain isomer (**C′**) to the bicylic isomer (**C**).

0947-6539/02/0824-5728 $ 20.00+.50/0 *Chem. Eur. J.* **2002**, *8*, No. 24

that the P–N and P–Cl bond lengths are reduced by 0.02–0.03 Å in going from a cc-pvdz basis to a cc-pvtz basis set. Changing the basis set has little effect on the N–P–N, P–N–P and N–P–Cl angles within **C′** and **C** optimised structures (R = H and CH_3). A direct comparison of experimental and theoretical structures is not possible since the subsitutents (R) differ, but comparing the B3LYP/cc-pvtz/R = CH_3 of the optimised isomer **C** with the experimental structure of bicyclic [$Cl_2P_4(\mu$-Npy$)_5$] (Table 3) shows a remarkable similarity in the P–N cage. P–N bond lengths are within 0.02 Å of agreement between theory and experimental data, with the B3LYP bonds lengths being longer. The N–P–N angles were calculated in the range 99.5–102.4°, the P–N–P angles were calculated in the range 123.4–129.4° and N–P–Cl mean was calculated to be 101.6°; these are all in close agreement with the angle parameters given in Table 3. The B3LYP/cc-pvtz model calculated a P–Cl bond length that is roughly 0.08 Å longer than given in Table 3.

Frequency analysis of the optimised structures obtained from all model and basis set combinations calculated for isomer **C′** (R = H and R = CH_3) gave minimum structures on the potential energy surface (PES). Care must be taken to ensure the methyl hydrogen atoms are in a staggered orientation for isomer **C′** otherwise in an eclipsed configuration, an imaginary frequency is obtained with the B3LYP/cc-pvtz optimised structure. This saddle point pertains to the oscillation of the methyl groups on the P–N cage, not the methyl on the bridge. For isomer **C** the frequency analysis was somewhat more complicated. For this isomer (R = H), an imaginary frequency was obtained for the optimised structures generated from the B3LYP/cc-pvdz and MP2/cc-pvdz models. Subsequent analysis of this structure confirmed it to be a transition state on the potential energy surface (PES). The bridged hydrogen oscillates along the Cl–H–Cl plane. The optimised structure obtained for isomer **C** (R = H) calculated from the B3LYP/cc-pvtz model produces a minimum on the PES. Minimum structures were confirmed, generated from the B3LYP/cc-pvdz and B3LYP/cc-pvtz models for isomer **C** (R = CH_3).

Table 4 details the ΔE, ΔH and ΔG for the isomer rearrangement (Scheme 7). The energetics are not presented for the BL3YP/cc-pvdz/R = H and MP2/cc-pvdz/R = H structures, since this would involve the reaction of a local minimum to a transition state on the PES, although the computed energies predict this would be a favourable rearrangement (**C′** → **C**). As outlined in Table 4, the energetics of the rearrangement of the chain isomer (**C′**) to the bicyclic isomer (**C**) are always favoured, although by increasing the size of the R group the process becomes less favourable; replacing hydrogen with a methyl group decreases ΔE by 9.1 kcal mol^{-1} while ΔG is lowered by 9.7 kcal mol^{-1} at the B3LYP/cc-pvtz level. Steric factors therefore appear to play an important role in this rearrangement, and it is reasonable to imagine that with even more sterically demanding substituents the energetic balance may be shifted further towards **C′**. In addition, although the entropy for the conversion of **C′** to **C** is calculated always to be unfavourable, as the size of the substituent increases from R = H to R = Me the entropy favours the chain isomer **C′** and disfavours the rearrangement.

Table 4. Energetics for isomer **C′** → **C** rearrangement.

C′ → **C**	ΔE[a, b]	ΔH[b, c]	ΔG[b, c]
B3LYP/cc-pvtz (R = H)	– 18.5	– 19.1	– 15.8
B3LYP/cc-pvdz (R = CH_3)	– 11.6	– 12.6	– 8.4
B3LYP/cc-pvtz (R = CH_3)	– 9.4	– 10.4	– 6.1

[a] Includes zero-point energy. [b] Units in kcal mol^{-1}. [c] At 298.15 K and 1 atm.

Conclusion

The study presented here has shown for the first time that dimers of the type [ClP(μ-NR)]$_2$, the commonest structural class of imidophospha(III)zanes, can be converted into bicyclic cages by a presumed "twist" mechanism. Placing this observation in the context of previous studies of other classes of imidophospha(III)zanes, it is possible to suggest a plausible mechanistic connection between the majority of structural types identified so far, which explains the observed dependence of the reactions on the steric demands of the organic substituents. This proposed scheme accounts for the observed selectivity between the macrocylic or adamantoid alternatives. In the broader context of our ongoing studies of larger macrocycles of the type [{P(μ-NR)}$_2$(μ-NH)]$_n$ ($n > 2$), one future prospect is the potential thermal rearrangement of these species by a similar mechanism to that involved in the conversion of **1** into **2**, or for the similar rearrangement of the dimeric macrocyle [{P(μ-N*i*Pr)$_2$(μ-N*i*Pr)]$_2$ into the adamantoid [P_4(N*i*Pr)$_6$]. Such a scenario is depicted in Scheme 8 for a tetrameric macrocyclic framework.

Experimental Section

PCl_3 was freshly distilled prior to use and stored under argon subsequently. Toluene and THF were dried by distillation over sodium/benzophenone under N_2 prior to the reactions. Compounds 2-amino-pyridine (2-pyNH_2) and 6-methyl-2-amino-pyridine (6-Me-2-pyNH_2) were used as supplied (Aldrich), without further purification. The products **1**, **2** and **4** were air- and moisture-sensitive. They were handled on a vacuum line using standard inert-atmosphere techniques[13] and under dry, oxygen-free argon. The products were isolated and characterised with the aid of a N_2-filled glove box fitted with a Belle Technology O_2 and H_2O internal recirculation system. Elemental analyses were performed by first sealing the samples under argon in air-tight aluminium boats (1–2 mg) and C, H and N content was analysed using an Exeter Analytical CE-440 Elemental Analyser. P analysis was performed by spectrophotometric means. ^{1}H and ^{31}P NMR spectra were recorded on a Bruker AM 400 MHz spectrometer in dry deuterated THF and/or benzene. ^{1}H NMR spectra were referenced to the internal solvent resonances. ^{31}P NMR spectra were referenced to an external standard of 85% H_3PO_4/D_2O.

Synthesis of 1 and 2: *n*BuLi (13.4 mL, 1.5 mol dm^{-3} in hexanes) was added to a solution of 2-pyNH_2 (1.882 g, 20 mmol) in THF (50 mL) at 0 °C. Warming of the mixture to room temperature and stirring for 15 mins gave a yellow solution of the lithiate. This solution was added dropwise to a solution of PCl_3 (1.75 mL, 20 mmol) in THF (60 mL) and Et_3N (5 mL) at – 78 °C. Immediate precipitation of a white solid occurred. The mixture was stirred at – 78 °C for a further 2 h after full addition of the lithiate, and then at room temperature for 12 h. The solvent was removed under vacuum and the yellow residue extracted with toluene (60 mL) and filtered (Celite, P3)

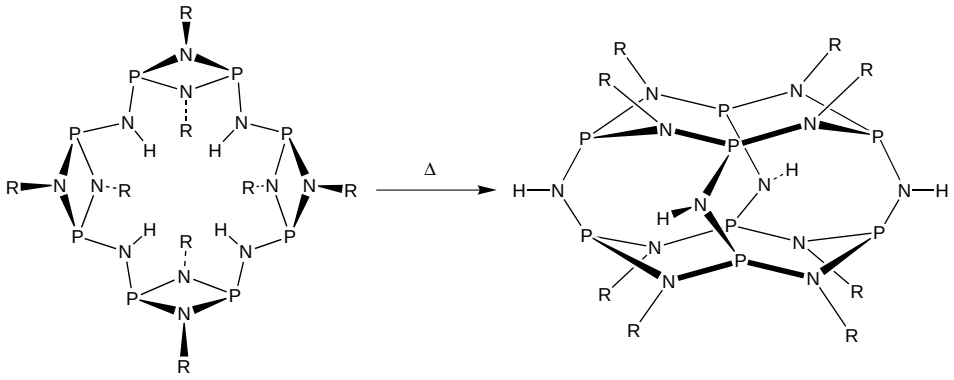

Scheme 8. Potential thermal rearrangement of a tetrameric macrocycle $[\{P(\mu\text{-NR})\}_2(\mu\text{-NH})]_4$.

to remove LiCl and Et_3NHCl. The toluene was removed completely under vacuum and the solid residue held under vacuum for 30 mins (10^{-1} torr) to remove volatile components. The solid was dissolved in toluene (6 mL) and heated into solution. Storage of the solution at room temperature (12 h) gave large yellow blocks of **1**. The first batch yield was 0.68 – 0.93 g (21 – 29 % on the basis of P supplied). Further crystallisation gave **2**·toluene as yellow rods, which were generally contaminated with small amounts of **1** (0.21 – 0.30 g).

Compound ***1***: M.p. 170 °C; IR (Nujol, NaCl): $\tilde{\nu} = 3050$ (w) (C–H str, aryl), 1587 (s) (C:N str), 1567 (s) (C:C str), other bands at 1295 (s), 1238 (s), 1154 (m), 1104 (m), 1050 (w), 994 (s), 944 (s), 921 (s), 778 (d.s), 734 (d.s), 690 cm^{-1} (d.s); ^1H NMR (400.16 MHz, $[D_6]$benzene, +25 °C): $\delta = 8.11$ (m, 1H; C(6)–H), 6.93 (m, 1H; C(5)–H), 6.42 (m, 2H; C(3,4)–H]; ^{31}P NMR (161.975 MHz, $[D_6]$benzene, +25 °C): $\delta = 178.5$ (s); MS (EI): *m*/*z*: 316.0 [MH^+] (50 %); elemental analysis calcd (%) for **1** (317.04): Cl 22.4, P 19.5; found: Cl 22.0, P 18.3.

Compound ***2***: M.p. 196 °C; IR (Nujol, NaCl): $\tilde{\nu} = 3055$ (w) (C–H str aryl), 1587 (s) (C–N str), 1570 (s) (C–C str), other bands at 1239 (s), 1150 (w), 1102 (w), 1047 (w), 997 (s), 972 (s), 939 (s), 921 (s), 908 (s), 889 (m), 776 (d.m), 730 cm^{-1} (m); ^1H NMR (400.16 MHz, $[D_6]$benzene, +25 °C): $\delta =$ 8.27 (m, 1H), 8.05 (m, 4H), 7.59 (d, 4H), 7.35 (d, 1H), 7.24 (m, 5H; $C_6H_5CH_3$), 7.12 (m, 8H), 6.98 (m, 2H), 2.19 (s, 3H; $C_6H_5CH_3$), the pairs of multiplets at 8.27/8.05, 7.59/7.35 and 7.12/6.98 have identical appearances; ^{31}P NMR (161.975 MHz, $[D_6]$benzene, +25 °C): $\delta = 108.4$ (t), 64.6 (t, $^2J(PNP) = 7.3$ Hz); elemental analysis calcd (%) for **2**·toluene (747.42): C 51.4, H 3.7, N 18.7, Cl 9.5, P 16.6; found: C 48.7, H 3.8, N 17.9, Cl 9.8, P 16.4.

Synthesis of 4: *n*BuLi (13.4 mL, 1.5 mol dm^{-3} in hexanes) was added to a solution of 6-Me-2-pyNH_2 (2.163 g, 20 mmol) in THF (40 mL) at 0 °C. Warming of the mixture to room temperature and stirring for 15 mins gave a yellow solution of the lithiate. This solution was added dropwise to a solution of PCl_3 (1.75 mL, 20 mmol) in THF (60 mL) and Et_3N (5 mL) at –78 °C. Immediate precipitation of a white solid occurred. The mixture was stirred at –78 °C for a further 2 h after full addition of the lithiate and then at room temperature for 12 h. The solvent was removed under vacuum and the yellow residue extracted with toluene (60 mL) and filtered (Celite, P3) to remove LiCl and Et_3NHCl. The solvent was removed under vacuum and a yellow precipitate was formed after removal of approximately 30 mL of toluene. The solid was dissolved by heating to approximately 70 °C. Storage of the solution at room temperature (12 h) gave large yellow rods of **4**. Removal of a further 10 mL of solvent and storage of the solution at room temperature gave a further batch of **4**. Total yield 1.01 g (29 %); M.p. 161 °C; IR (Nujol, NaCl): $\tilde{\nu} = 1594$ (s) (C:N str), 1570 (s) (C:N str), other bands at 1255 (s), 1241 (s), 1234 (m), 1166 (s), 1159 (s), 1095 (s), 1060 (m), 994 (s), 964 (s), 925 (m), 824 (s), 807 (m), 785 (m), 782 cm^{-1} (m); ^1H NMR (400.16 MHz, $[D_6]$benzene, +25 °C): $\delta = 6.91$ (t, $J(H,H) = 7.4$ Hz, 1H; C(4)–H), 6.28 (dd, $J(H,H) = 2.6$, 7.8 Hz, 2H; C(3,5)–H), 2.23 (s, 3H; Me); ^{31}P NMR (161.975 MHz, $[D_6]$benzene, +25 °C): $\delta = 183.3$ (s); elemental analysis calcd (%) for **4** (345.10): C 41.8, H 3.5, N 16.2, Cl 20.6, P 18.0; found: C 38.2, H 3.6, N 15.4, Cl 19.8, P 17.6.

X-ray crystallographic studies of 1, 2·toluene and 4: Crystals of **1**, **2** and **4** were mounted directly from solution under argon using an inert oil which protected them from atmospheric oxygen and moisture.[14] X-ray intensity data were collected using a Bruker P4 four-circle diffractometer (for **1** and **2**) or a Nonius Kappa CCDC diffractometer (for **4**). Details of the data collections and structural refinements are given in Table 1. The structures were solved by direct methods and refined by full-matrix least squares on F^2.[15] Atomic coordinates, bond lengths and angles and thermal parameters for **1**, **2** and **4** have been deposited with the Cambridge Crystallographic Data Centre.

CCDC-188038 (**1**), -188039 (**2**·toluene) and -188040 (**3**) contain the supplementary crystallographic data for this paper. These data can be obtained free of charge via www.ccdc.cam.ac.uk/conts/retrieving.html (or from the Cambridge Crystallographic Data Centre, 12 Union Road, Cambridge CB2 1EZ, UK; fax: (+44) 1223-336-033; or e-mail: deposit@ccdc.cam.ac.uk).

Acknowledgements

We gratefully acknowledge the EPSRC (A.B., E.M.D., F.G., G.T.L., D.J.L., M.McP., D.S.W.), St. Catharine's College Cambridge (Fellowship for A.D.W.) and the Cambridge European Trust (F.G.) for financial support. D.M. acknowledges the support of the Office of Energy Research, Office of Basic Energy Sciences, Division of Chemical Sciences, US Department of Energy under Grant DE-FG02-97ER-14758.

[1] For structurally characterised examples, see: a) K. Muir, *J. Chem. Soc. Dalton Trans.* **1975**, 259; b) H.-J. Chen, R. C. Haltiwanger, T. G. Hill, M. L. Thomson, D. E. Coons, A. D. Norman, *Inorg. Chem.* **1985**, *24*, 4725; c) V. D. Romanenko, A. D. Drapailo, A. N. Chernega, L. N. Markovskii, *Zh. Obshch. Khim.* **1991**, *61*, 2434; d) J.-T. Ahlemann, H. W. Roesky, R. Murugavel, E. Parisini, M. Noltemeyer, H.-G. Schmidt, O. Müller, R. Herbst-Irmer, L. N. Markovskii, Y. G. Shermobich, *Chem. Ber.* **1997**, *130*, 1113; e) P. B. Hitchcock, M. F. Lappert, M. Layh, *J. Organomet. Chem.* **1997**, *529*, 243.

[2] a) R. Jefferson, J. F. Nixon, T. M. Painter, *J. Chem. Soc. Chem. Commun.* **1969**, 622; b) W. Zeiss, K. Barlos, *Z. Naturforsh. B* **1979**, *34*, 423; c) D. A. Harvey, R. Keat, D. S. Rycroft, *J. Chem. Soc. Dalton Trans.* **1983**, 425.

[3] a) R. Murugavel, S. S. Krishnamurthy, M. Nethaji, *J. Chem. Soc. Dalton Trans.* **1993**, 2569; b) N. Thirupathi, S. S. Krishnamurthy, M. Nethaji, *J. Chem. Soc. Dalton Trans.* **1998**, 1469.

[4] R. R. Holmes, J. A. Forstner, *Inorg. Chem.* **1963**, *2*, 380; J. Navech, J.-P. Majoral, *Phosphorus Sulfur Silicon Relat. Elem.* **1983**, *15*, 51.

[5] a) O. J. Scherer, K. Andres, C. Krüger, Y.-H. Tsay, G. Wolmerhäuser, *Angew. Chem.* **1980**, *92*, 563; *Angew. Chem. Int. Ed. Engl.* **1980**, *19*, 571; b) J. K. Brask, T. Chivers, M. Krahn, M. Parvez, *Inorg. Chem.* **1999**, *38*, 290.

[6] W. Zeiss, W. Endrass, *Z. Naturforsch. B* **1979**, *34*, 678.

[7] A. Bashall, E. L. Doyle, C. Tubb, S. J. Kidd, M. McPartlin, A. D. Woods, D. S. Wright, *Chem. Commun.* **2001**, 2542.

[8] A. Bashall, E. L. Doyle, C. Tubb, S. J. Kidd, M. McPartlin, M. Parry, A. D. Woods, D. S. Wright, *Chem. Eur. J.* **2002**, *8*, 3377.

[9] Gaussian 98 (Revision A.11.2), M. J. Frisch, G. W. Trucks, H. B. Schlegel, G. E. Scuseria, M. A. Robb, J. R. Cheeseman, V. G. Zakrzewski, J. A. Montgomery, Jr., R. E. Stratmann, J. C. Burant, S. Dapprich, J. M. Millam, A. D. Daniels, K. N. Kudin, M. C. Strain, O. Farkas, J. Tomasi, V. Barone, M. Cossi, R. Cammi, B. Mennucci, C. Pomelli, C. Adamo, S. Clifford, J. Ochterski, G. A. Petersson, P. Y. Ayala, Q. Cui, K. Morokuma, N. Rega, P. Salvador, J. J. Dannenberg, D. K. Malick, A. D. Rabuck, K. Raghavachari, J. B. Foresman, J. Cioslowski, J. V. Ortiz, A. G. Baboul, B. B. Stefanov, G. Liu, A. Liashenko, P. Piskorz, I. Komaromi, R. Gomperts, R. L. Martin, D. J. Fox, T. Keith, M. A. Al-Laham, C. Y. Peng, A. Nanayakkara, M.

  0947-6539/02/0824-5730 $ 20.00+.50/0

Challacombe, P. M. W. Gill, B. Johnson, W. Chen, M. W. Wong, J. L. Andres, C. Gonzalez, M. Head-Gordon, E. S. Replogle, J. A. Pople, Gaussian, Inc., Pittsburgh, PA, **2001**.
[10] A. D. Becke, *J. Chem. Phys.* **1993**, *104*, 1040.
[11] T. H. Dunning, *J. Chem. Phys.* **1989**, *90*, 1007.
[12] D. E. Woon, T. H. Dunning, *J. Chem. Phys.* **1993**, *98*, 1358.
[13] D. F. Shriver, M. A. Drezdon, *The Manipulation of Air-Sensitive Compounds*, 2nd ed., Wiley, New York, **1986**.
[14] T. Kottke, D. Stalke, *J. Appl. Crystallogr.* **1993**, *26*, 615.
[15] G. M. Sheldrick, SHELXL97, University of Göttingen, Göttingen (Germany), **1997**.

Received: June 21, 2002 [F4197]

  0947-6539/02/0824-5731 $ 20.00+.50/0